particles

MDPI

Article

LHC Search Strategy for Squarks in Higgsino-LSP Scenarios with Leptons and *b*-Jets in the Final State

Ernesto Arganda [1,2,*], Antonio Delgado [3], Roberto A. Morales [2] and Mariano Quirós [4]

[1] Instituto de Física Teórica UAM-CSIC, C/Nicolás Cabrera 13-15, Campus de Cantoblanco, 28049 Madrid, Spain
[2] IFLP, CONICET—Dpto. de Física, Universidad Nacional de La Plata, C.C. 67, La Plata 1900, Argentina; roberto.morales@fisica.unlp.edu.ar
[3] Department of Physics, University of Notre Dame, 225 Nieuwland Hall, Notre Dame, IN 46556, USA; adelgad2@nd.edu
[4] Institut de Física d'Altes Energies (IFAE) and BIST, Campus UAB, Bellaterra, 08193 Barcelona, Spain; quiros@ifae.es
* Correspondence: ernesto.arganda@csic.es

Abstract: The higgsino Lightest Supersymmetric Particle (LSP) scenario opens up the possibility of decays of strongly produced particles to an intermediate neutralino, due to the Yukawa-suppressed direct decays to the higgsino. Those decays produce multijet signals with a Higgs or a Z boson being produced in the decay of the intermediate neutralino to the LSP. In this paper, we study the discovery prospects of squarks that produce b-jets and leptons in the final state. Our collider analysis provides signal significances at the 3σ level for luminosities of 1 ab^{-1}, and at the 5σ level if we project these results for 3 ab^{-1}.

Keywords: LSP higgsino at LHC; higgsino dark matter; supersymmetric LHC searches

Citation: Arganda, E.; Delgado, A.; Morales, R.A.; Quirós, M. LHC Search Strategy for Squarks in Higgsino-LSP Scenarios with Leptons and *b*-Jets in the Final State. *Particles* **2022**, *5*, 265–272. https://doi.org/10.3390/particles5030023

Academic Editor: Armen Sedrakian

Received: 23 June 2022
Accepted: 15 July 2022
Published: 19 July 2022

1. Introduction

The hierarchy problem and the existence of dark matter (DM) are two of the strongest motivations to enlarge the Standard Model (SM) with low energy R-parity conserving supersymmetry (MSSM) [1–5]. One of the consequences is the stability of the LSP, and hence a possible DM candidate. One appealing possibility to avoid the constraints coming from direct detection experiments is to assume that the higgsino is the LSP [6], and its implementation in the MSSM as done in [7].

Building on the intuition and knowledge gained in our previous works [8–10] on the LHC phenomenology of MSSM scenarios with higgsino-LSP, and taking into account the large number of events that we could expect at 14 TeV and 300 fb^{-1} for the production of squark pairs [10], we consider in this work that the bino-like neutralino decays into the higgsino-LSP plus a leptonic Z boson as another interesting decay channel. This feature implies, on the one hand, the reduction of expected signal events; however, on the other hand, it will provide a better control of all backgrounds, especially for discarding the QCD multijet background.

We now summarize our previous work on related subjects. We have studied the gluino pair production with subsequent decays into the bino-like neutralino plus two jets, then decaying into the LSP plus the Higgs boson resulting in a final state of four light-jets, four b-jets and large amount of missing energy [8]. Another interesting signature for gluino pair production was presented in [9] with $4j + 2\tau + E_T^{\rm miss}$ final state. Finally, we studied the pair production of squark with decays resulting in 2 light-jets, two Higgs bosons (decaying into $b\bar{b}$) plus missing energy in the final state (also with the bino-like neutralino as intermediate state in the SUSY cascade) in [10].

This paper is organized as follows: in Section 2 we present the details of the event simulation and develop our search strategy by means of the characterization of the signal

against the background, and Section 3 is devoted to the discussion of our main results and a summary of the most important conclusions.

2. Simulation and Collider Analysis

The signal and backgrounds were generated with MadGraph_aMC@NLO 2.8.1 [11] for a center-of-mass energy of $\sqrt{s}$ = 14 TeV. The events are showered and hadronized using PYTHIA 8.2 [12], and the detector effects are implemented with Delphes 3.3.3 [13]. We consider a working point for the efficiency of b-tagging of 0.75, with a rate of misidentification of 0.01 for light-jets and 0.1 for c-jets. The internal analysis codes and simulation input files are available upon request to authors.

The relevant signature for this work is represented in Figure 1, which corresponds to first-generation squark-pair production followed by the decay into a bino-like $\tilde{\chi}_3^0$ plus a light jet. Then, one $\tilde{\chi}_3^0$ decays into the higgsino-like LSP and the SM-like Higgs boson (decaying into $b\bar{b}$). To reduce the QCD backgrounds, we consider that the other $\tilde{\chi}_3^0$ decays into the LSP plus a Z boson decaying into e^+e^- or $\mu^+\mu^-$ pairs. We study the same supersymmetric spectra as in our previous work [10], which is not excluded by the validated analyses of `CheckMATE 2.0.24` [14] (We have canvassed searches with higher luminosity and we have found no analysis that would exclude our spectrum). Within these higgsino-LSP MSSM scenarios, in which we vary M_1 from 600 to 800 GeV and fix $M_2 = 3$ TeV, $M_3 = 2.2$ TeV and $\mu = 0.5$ TeV, one has BR($\tilde{\chi}_3^0 \to \tilde{\chi}_{1,2}^0 h$)∼BR($\tilde{\chi}_3^0 \to \tilde{\chi}_{2,1}^0 Z$) but the lower BR($Z \to l^- l^+$) = 6.7% ($l = e, \mu$) with respect to BR($h \to b\bar{b}$) = 58% is compensated for by a cleaner final state than in our previous work, yielding to a complementary channel to these spectra. On the other hand, the production cross section of the signal is obtained from [15], in which NLO and NLL QCD corrections are included. We define two production cases corresponding to both $pp \to \tilde{u}_L \tilde{u}_L$ and $pp \to \tilde{d}_L \tilde{d}_L$ (*Left* case), and to $pp \to \tilde{u}_R \tilde{u}_R$ (*Right* case).

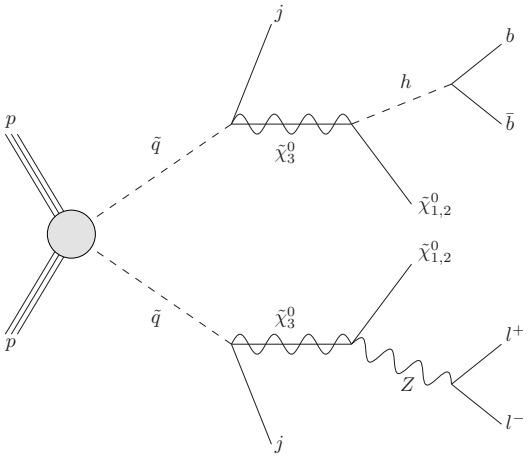

Figure 1. Representative Feynman diagram corresponding to our signature with $2l + 2b + 2j + E_T^{\text{miss}}$ in the final state.

Concerning the experimental bounds on our MSSM scenarios, we have not found any LHC search with the same final state and similar spectra. As far as we know, the most related analysis to our study would be [16,17]. However, in these works, it is assumed that there are only Higgs bosons in the electroweak production and with a massless gravitino. Moreover, for colored-particle production, no b-tagging is done, and it is assumed that the decay of the second neutralino is via a Z boson without Higgs bosons. Therefore, our proposed MSSM scenarios evade again such exclusion limits. In addition, our comparison with `CheckMATE` gives [18] as the most sensitive search (but very far from the exclusion) for its signal region $SRI - MLL - 60$ when looking for compressed supersymmetric spectra with leptons and missing transverse momentum in the final state (but no b-jets). Finally, supersymmetric signatures with leptons, b-jets, and missing energy are produced by top

squarks; see for instance [19], thus they are not sensitive to our signature with Higgs and Z bosons.

The relevant backgrounds are $t\bar{t}$+jets and $t\bar{t}$ production in association with a vector boson. The leptons coming from the Z-boson decay in the signature reject the presence of the QCD multijet background in this analysis. We then consider the following SM backgrounds: the fully leptonic decay of $t\bar{t}$ pair up to one additional light jet, $t\bar{t}_{\rm lep} + j$ (inc.); the hadronic decay of $t\bar{t}$ in association with a leptonic Z boson, $t\bar{t}_{\rm had} + Z$; the semileptonic decay of $t\bar{t}$ with a leptonic Z boson, $t\bar{t}_{\rm semilep} + Z$; and the semileptonic decay of $t\bar{t}$ in association with a leptonic W boson, $t\bar{t}_{\rm semilep} + W$. The jet matching and merging is performed by the MLM algorithm [20,21] using xqcut = 20 for all generated samples and `qcut` equal to 50 and 250 for backgrounds and signal, respectively.

We demand two b-jets and two opposite-sign (OS) same-flavor leptons (electrons or muons) at reconstructed level:

$$\text{Selection cuts: } N_b = 2 \text{ and } N_{\rm lep}^{\rm OS} = 2\,. \tag{1}$$

To optimize our background simulation, we display in Figure 2 the transverse momentum of the second leading lepton $p_T^{2^{nd}\,lep}$ (left panel), the second leading b-jet $p_T^{2^{nd}\,b}$ (right panel) and, in Figure 3, the missing transverse energy $E_T^{\rm miss}$ over samples of signal and backgrounds without parton-level cuts. We conclude from these three distributions that the parton-level cuts of $p_T^b > 25$ GeV, $p_T^{lep} > 25$ GeV and $E_T^{\rm miss} > 200$ GeV applied to the background simulation reduce the large cross-sections and the event generation becomes more efficient. With this setup, the cross-sections of the $t\bar{t}_{\rm lep} + j$ (inc.), $t\bar{t}_{\rm had} + Z$, $t\bar{t}_{\rm semilep} + Z$, and $t\bar{t}_{\rm semilep} + W$ backgrounds are 1.1×10^3, 19.42, 0.53 and 0.83 fb, respectively.

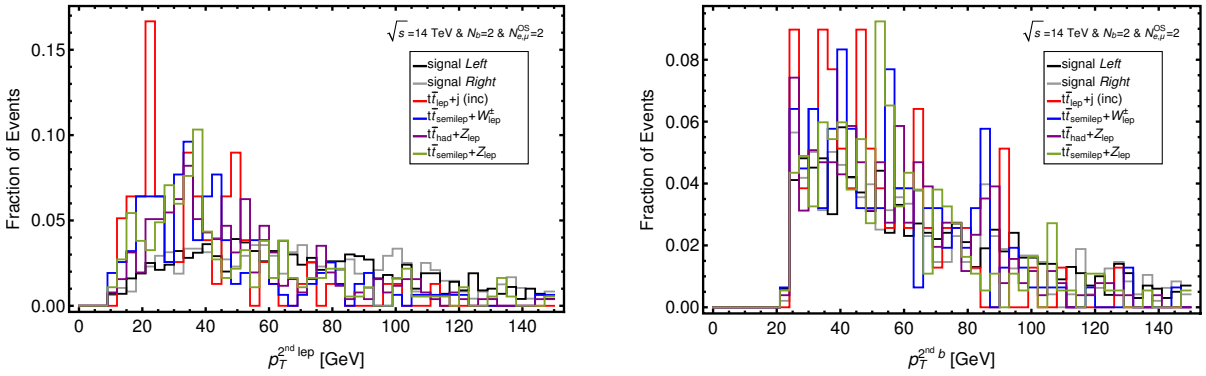

Figure 2. Distributions of transverse momentum of the second leading lepton $p_T^{2^{nd}\,lep}$ (**left** panel) and second leading b-jet $p_T^{2^{nd}\,b}$ (**right** panel) over samples of signal and backgrounds without parton-level cuts.

On the other hand, the invariant mass of a pair of OS leptons m_{ll} and a pair of b-jets m_{bb} are shown in the left and right panels of Figure 4. Then it is natural to demand values of these kinematical variables in a 10% window around the Z and Higgs boson mass, respectively.

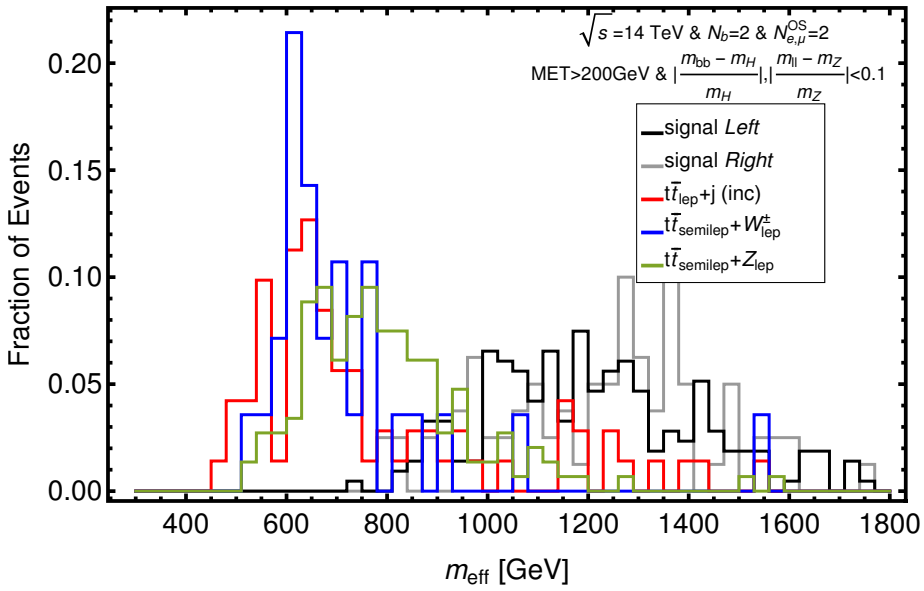

Figure 3. Distribution of missing energy E_T^{miss} over samples of signal and backgrounds without parton-level cuts.

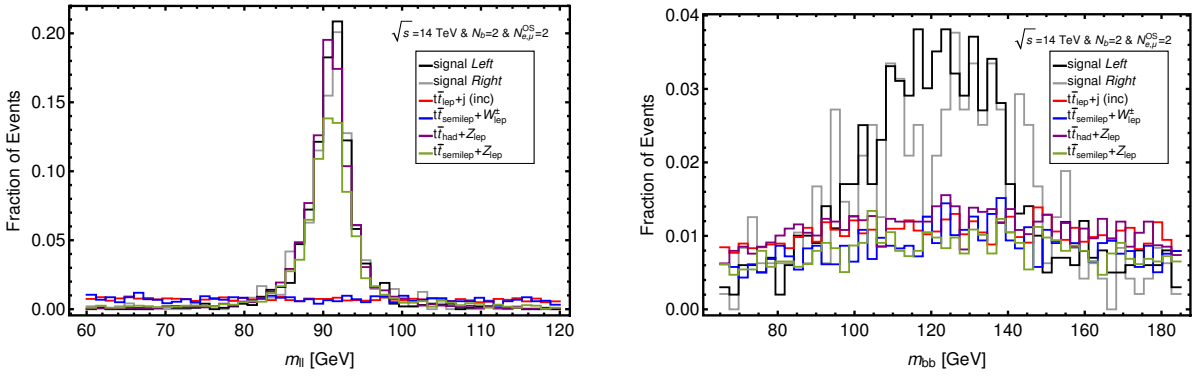

Figure 4. Distributions of the invariant mass of a pair of OS leptons m_{ll} (**left** panel) and a pair of b-jets m_{bb} (**right** panel) over samples of signal and backgrounds without parton-level cuts.

Therefore, we applied at detector level the following cuts:

$$p_T^{lep} > 25 \text{ GeV}, \, p_T^b > 25 \text{ GeV and } E_T^{\text{miss}} > 200 \text{ GeV}, \tag{2}$$

and

$$\left|\frac{m_{ll} - m_Z}{m_Z}\right| < 0.1 \text{ and } \left|\frac{m_{bb} - m_h}{m_h}\right| < 0.1. \tag{3}$$

We develop a search strategy for a luminosity of $\mathcal{L} = 1$ ab^{-1}, corresponding to the high luminosity LHC phase (HL-LHC), and optimize our analysis for a benchmark with squark masses of 1 TeV for both *Left* and *Right* productions. After requiring Equations (1)–(3), the $t\bar{t}_{\text{had}} + Z$ background disappears. To mostly reduce the backgrounds with leptons and missing transverse energy coming from the W boson, we resort to the transverse mass of the second leading lepton $\vec{p}^{\,2^{nd}\,lep}$ and the missing momentum $\vec{p}_T^{\,\text{miss}}$ given by

$$m_T^{2^{nd}\,lep} \equiv m_T(\vec{p}^{\,2^{nd}\,lep}, \vec{p}_T^{\,\text{miss}}) = \sqrt{2p_T^{2^{nd}\,lep} E_T^{\text{miss}} (1 - \cos\Delta\phi(\vec{p}^{\,2^{nd}\,lep}, \vec{p}_T^{\,\text{miss}}))}\,. \tag{4}$$

We also consider the effective mass variable m_{eff} corresponding to the scalar sum of the missing energy and the transverse momentum of all reconstructed objects. Figure 5 shows the distributions of these two variables after demand the cuts of Equations (1)–(3).

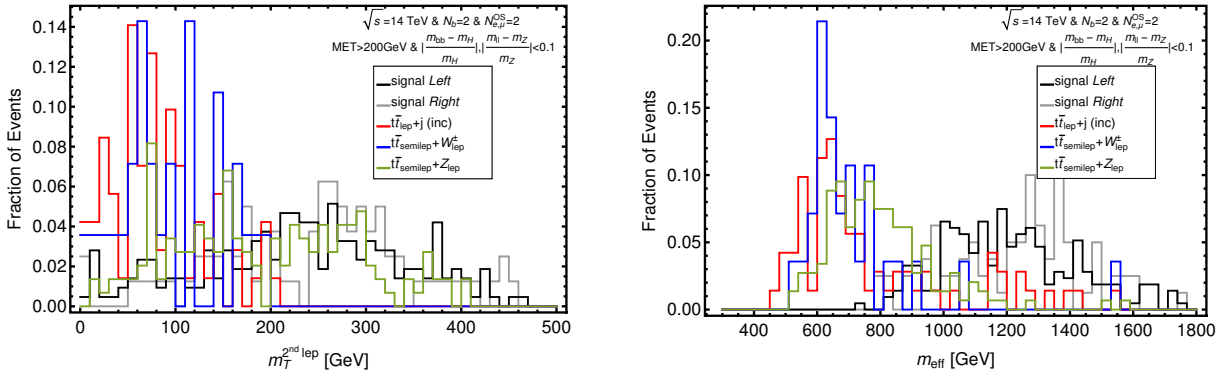

Figure 5. Distributions of the transverse mass of the second lepton $m_T^{2^{nd}\,lep}$ (**left**) and the effective mass m_{eff} (**right**), for signal and background after requiring two b-jets, two OS leptons and satisfying Equations (1)–(3).

We can see from the left panel of Figure 5 that the $t\bar{t}_{\text{lep}} + j$ (inc.) and $t\bar{t}_{\text{semilep}} + W^{\pm}$ backgrounds have values below 220 GeV for this variable. From the effective mass distributions, we found that background peaks are below 1000 GeV while the signal have most of its events above this value.

To obtain an estimate of the LHC sensitivity to our SUSY signal, we use the following expression for the signal significance, including background systematic uncertainties [22,23]:

$$\mathcal{S} = \sqrt{2\left((B+S)\log\left(\frac{(S+B)(B+\sigma_B^2)}{B^2+(S+B)\sigma_B^2}\right) - \frac{B^2}{\sigma_B^2}\log\left(1+\frac{\sigma_B^2 S}{B(B+\sigma_B^2)}\right)\right)}, \tag{5}$$

where S (B) is the number of signal (background) events and $\sigma_B = (\Delta B)B$, with ΔB being the relative systematic uncertainty chosen to be a conservative value of 30%.

3. Discussion and Summary

The resulting cut flows for both *Left* and *Right* signal cases are presented in Tables 1 and 2, respectively, in which the different cuts that define our search strategy are listed. First we can observe that the selection cuts are very useful to drastically reduce the $t\bar{t}_{\text{lep}} + j$ background, which is potentially the most problematic, and whose number of events drops by two orders of magnitude after these cuts, while the number of events of the rest of the backgrounds and signal are reduced by about one order of magnitude. The cuts of Equations (2)–(3) remove all $t\bar{t}_{\text{had}} + Z$ background events and reduce two orders of magnitude of the rest, while the signal events decrease less than one order of magnitude. After the $m_T^{2^{nd}lep}$ cut, only the $t\bar{t}_{\text{semilep}} + Z$ background survives, and the signal is hardly affected. Finally, the m_{eff} cut helps to further reduce the $t\bar{t}_{\text{semilep}} + Z$ background with little change in the number of final signal events. At the end, for a total integrated luminosity of $\mathcal{L} = 1$ ab^{-1}, we expect signal significances of 4.02σ and 2.61σ for the *Left* and *Right* cases, respectively. If we project these results for a luminosity of 3 ab^{-1}, the significances would reach values of 6.65σ and 4.37σ, respectively, that one can consider at the discovery level of sensitivity. For this projection, we assume in a conservative way that the background rates scale as the cross section of the signal. In addition, the zeros in the last row of Tables 1 and 2 must be interpreted as the projection of our vanishing simulated samples to $\mathcal{L} = 1$ ab^{-1}.

Table 1. Cut flow with $\mathcal{L} = 1$ ab^{-1} corresponding to the *Left* case signal production. The last column is the significance with a systematic uncertainty in the background of 30%. The last row is the projection to $\mathcal{L} = 3$ ab^{-1}.

Process	signal	$t\bar{t}_{\text{lep}} + j$ (inc.)	$t\bar{t}_{\text{had}} + Z$	$t\bar{t}_{\text{semilep}} + Z$	$t\bar{t}_{\text{semilep}} + W^{\pm}$	$\mathcal{S}$
Expected	239	1.11×10^6	19,420	530	830	7×10^{-4}
selection cut	29.8	40,888	2140	38	39	2.3×10^{-3}
cuts of Equations (2)–(3)	5.9	200	0	1.6	0.27	0.09
$m_T^{2^{nd}lep} > 220$ GeV	3.7	0	0	0.86	0	2.61
$m_{eff} > 1000$ GeV	3.4	0	0	0.11	0	4.02
$\mathcal{L} = 3$ ab^{-1}	10.2	0	0	0.33	0	6.65

Table 2. Cut flow with $\mathcal{L} = 1$ ab^{-1} corresponding to the *Right* case signal production. The last column is the significance with a systematic uncertainty in the background of 30%. The last row is the projection to $\mathcal{L} = 3$ ab^{-1}.

Process	signal	$t\bar{t}_{\text{lep}} + j$ (inc.)	$t\bar{t}_{\text{had}} + Z$	$t\bar{t}_{\text{semilep}} + Z$	$t\bar{t}_{\text{semilep}} + W^{\pm}$	$\mathcal{S}$
Expected	195	1.11×10^6	19,420	530	830	5.7×10^{-4}
selection cut	23.4	40,888	2140	38	39	1.8×10^{-3}
cuts of Equations (2)–(3)	3.5	200	0	1.6	0.27	0.06
$m_T^{2^{nd}lep} > 220$ GeV	2.3	0	0	0.86	0	1.76
$m_{eff} > 1000$ GeV	1.76	0	0	0.11	0	2.61
$\mathcal{L} = 3$ ab^{-1}	5.3	0	0	0.33	0	4.37

The promising results in Tables 1 and 2, for the higgsino-LSP MSSM benchmarks with squark masses of 1 TeV, encourage the extension of our analysis to other values of the parameter space of interest, defined in the plane $[M_{\tilde{q}}, M_{\tilde{\chi}_3^0}]$.

We show in Figure 6 the contour lines in the plane $[M_{\tilde{q}}, M_{\tilde{\chi}_3^0}]$ for $\tilde{q}_L$ (left panel) and $\tilde{u}_R$ (right panel) pair productions. The solid (dotted) lines correspond to a luminosity of $\mathcal{L} = 1$ (3) ab^{-1}. The brown, red, and blue colors represent the values of 2σ, 3σ and 5σ, respectively, for the signal significance, $\mathcal{S}$. For the lowest luminosity of 1 ab^{-1}, we are able to obtain 2σ significances, in the *Left* case, for virtually any $M_{\tilde{q}_L}$ value within the range considered [850 GeV–1100 GeV] and bino mass values above ∼650 GeV and below ∼850 GeV. One would reach significances at the evidence level for values of $M_{\tilde{q}_L} < 1050$ GeV and $M_{\tilde{\chi}_3^0}$ between 700 GeV and 850 GeV. This same area defines the discovery-level sensitivity for $\mathcal{L} = 3$ ab^{-1} in the *Left* case. Our search strategy, applied to the *Right* case, allows the obtaining of 2σ significances for $M_{\tilde{u}_R} \gtrsim 825$ GeV and practically any value of $M_{\tilde{\chi}_3^0}$ for $\mathcal{L} = 1$ ab^{-1}. Evidence-level significances are obtained in this case for $M_{\tilde{\chi}_3^0} \gtrsim 800$ GeV and $M_{\tilde{u}_R}$ values between 950 GeV and 1000 GeV. These squark and bino mass values also delimit the discovery-level area in the *Right* case for $\mathcal{L} = 3$ ab^{-1}.

To summarize, we have developed a search strategy for pairs of squarks at the HL-LHC, which both decay into bino neutralinos plus a jet. In turn, one of the binos decays into a Higgs boson plus the LSP, while the other decays into the LSP and a leptonic Z boson, which allows us to keep all backgrounds under control and to smoothly discard the QCD multijet background. Our collider analysis provides signal significances at the evidence level for luminosities of 1 ab^{-1} and at the discovery level if we project these results for 3 ab^{-1}. Together with our previous works [8–10], these complementary analyses represent a proof of principle of searches that are sensitive to spectra such that the gluino ([8,9]) or the first-generation squarks ([10] and this manuscript) do not directly decay to the LSP but

to an intermediate electroweakino that produces Higgs or Z bosons in its subsequent decay. Therefore, those spectra would escape current experimental searches.

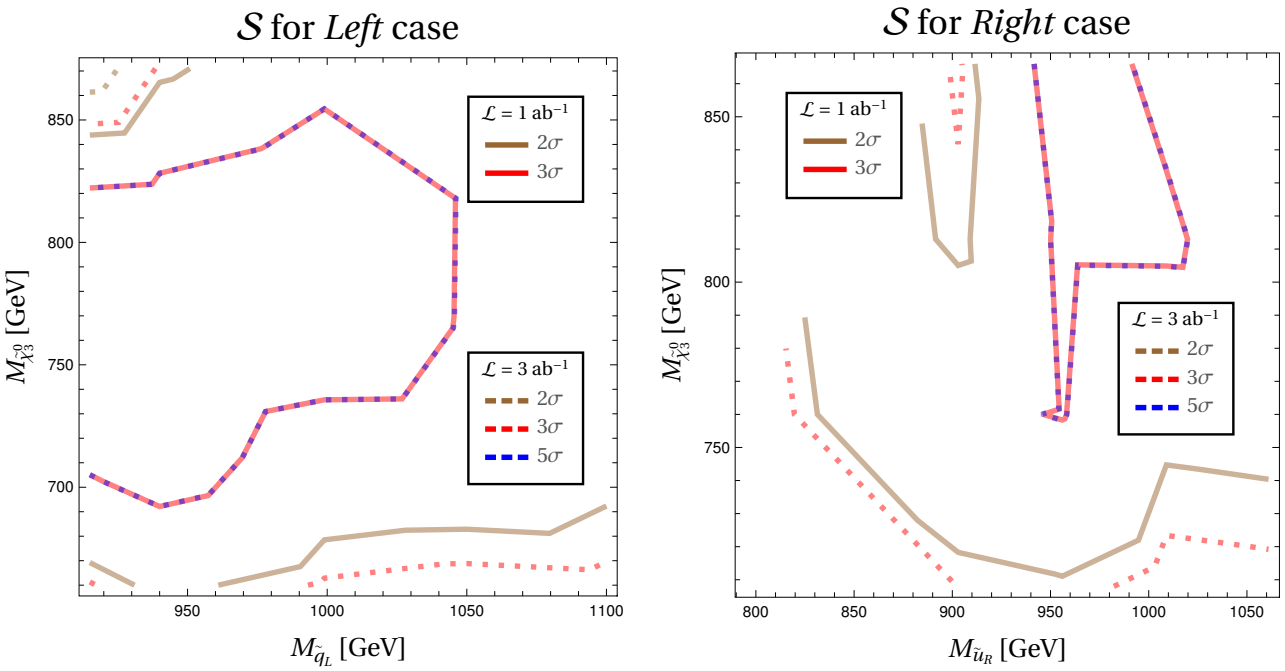

Figure 6. Contour lines in the plane $[M_{\tilde{q}}, M_{\tilde{\chi}_3^0}]$ for $\tilde{q}_L$ (**left**) and $\tilde{u}_R$ (**right**) productions. Solid (dotted) lines correspond to $\mathcal{L}$ = 1 (3) ab^{-1}. The brown, red and blue colors are the $\mathcal{S}$ (background systematic uncertainty of 30%) with values of 2σ, 3σ and 5σ, respectively.

Author Contributions: Writing—review & editing, E.A., A.D., R.A.M. and M.Q. All authors have read and agreed to the published version of the manuscript.

Funding: This research was funded by the "Atracción de Talento" program (Modalidad 1) of the Comunidad de Madrid (Spain) under grant number 2019-T1/TIC-14019; by the Spanish Research Agency (Agencia Estatal de Investigación) through the Grant IFT Centro de Excelencia Severo Ochoa No CEX2020-001007-S; by MCIN/AEI/10.13039/501100011033; by CONICET and ANPCyT (Argentina) under projects PICT 2017-2751 and PICT 2018-03682; by the National Science Foundation under grant PHY-2112540; by CONICET and ANPCyT under projects PICT 2016-0164, PICT 2017-2751 and PICT 2018-03682; by Spanish MINEICO under Grant FPA2017-88915-P; by the Catalan Government under Grant 2017SGR1069.

Data Availability Statement: Used https://twiki.cern.ch/twiki/bin/view/CMSPublic/PhysicsResultsSUS (20 March 2022) (CMS) and also https://twiki.cern.ch/twiki/bin/view/AtlasPublic/SupersymmetryPublicResults (20 March 2022) (ATLAS) data.

Acknowledgments: The work of EA is partially supported by the "Atracción de Talento" program (Modalidad 1) of the Comunidad de Madrid (Spain) under the grant number 2019-T1/TIC-14019, by the Spanish Research Agency (Agencia Estatal de Investigación) through the Grant IFT Centro de Excelencia Severo Ochoa No CEX2020-001007-S, funded by MCIN/AEI/10.13039/501100011033, and by CONICET and ANPCyT (Argentina) under projects PICT 2017-2751 and PICT 2018-03682. The work of AD was partially supported by the National Science Foundation under grant PHY-2112540. The work of RM is supported by CONICET and ANPCyT under projects PICT 2016-0164, PICT 2017-2751 and PICT 2018-03682. The work of MQ is partly supported by Spanish MINEICO under Grant FPA2017-88915-P, and by the Catalan Government under Grant 2017SGR1069. IFAE is partially funded by the CERCA program of the Generalitat de Catalunya.

Conflicts of Interest: The authors declare no conflict of interest.

References

1. Fayet, P. Supersymmetry and Weak, Electromagnetic and Strong Interactions. *Phys. Lett. B* **1976**, *64*, 159. [CrossRef]
2. Fayet, P. Spontaneously Broken Supersymmetric Theories of Weak, Electromagnetic and Strong Interactions. *Phys. Lett. B* **1977**, *69*, 489. [CrossRef]
3. Nilles, H.P. Supersymmetry, Supergravity and Particle Physics. *Phys. Rept.* **1984**, *110*, 1–162. [CrossRef]
4. Haber, H.E.; Kane, G.L. The Search for Supersymmetry: Probing Physics Beyond the Standard Model. *Phys. Rept.* **1985**, *117*, 75–263. [CrossRef]
5. Gunion, J.; Haber, H.E. Higgs Bosons in Supersymmetric Models. 1. *Nucl. Phys. B* **1986**, *272*, 1. Erratum: *Nucl. Phys. B* **1993**, *402*, 567–569. [CrossRef]
6. Kowalska, K.; Sessolo, E.M. The discreet charm of higgsino dark matter—A pocket review. *Adv. High Energy Phys.* **2018**, *2018*, 6828560. [CrossRef]
7. Delgado, A.; Quirós, M. Higgsino Dark Matter in the MSSM. *Phys. Rev. D* **2021**, *103*, 015024. [CrossRef]
8. Arganda, E.; Delgado, A.; Morales, R.A.; Quirós, M. Novel Higgsino dark matter signal interpretation at the LHC. *Phys. Rev. D* **2021**, *104*, 055003. [CrossRef]
9. Arganda, E.; Delgado, A.; Morales, R.A.; Quirós, M. Search strategy for gluinos at the LHC with a Higgs boson decaying into tau leptons. *arXiv* **2021**, arXiv:2107.06034.
10. Arganda, E.; Delgado, A.; Morales, R.A.; Quirós, M. Hunting Squarks in Higgsino LSP scenarios at the LHC. *arXiv.* **2021**, arXiv:2112.09198.
11. Alwall, J.; Frederix, R.; Frixione, S.; Hirschi, V.; Maltoni, F.; Mattelaer, O.; Shao, H.S.; Stelzer, T.; Torrielli, P.; Zaro, M. The automated computation of tree-level and next-to-leading order differential cross sections, and their matching to parton shower simulations. *JHEP* **2014**, *7*, 79. [CrossRef]
12. Sjöstrand, T.; Ask, S.; Christiansen, J.R.; Corke, R.; Desai, N.; Ilten, P.; Mrenna, S.; Prestel, S.; Rasmussen, C.O.; Skands, P.Z. An Introduction to PYTHIA 8.2. *Comput. Phys. Commun.* **2015**, *191*, 159–177. [CrossRef]
13. de Favereau, J.; Delaere, C.; Demin, P.; Giammanco, A.; Lemaître, V.; Mertens, A.; Selvaggi, M. DELPHES 3, A modular framework for fast simulation of a generic collider experiment. *JHEP* **2014**, *2*, 057. [CrossRef]
14. Dercks, D.; Desai, N.; Kim, J.S.; Rolbiecki, K.; Tattersall, J.; Weber, T. CheckMATE 2: From the model to the limit. *Comput. Phys. Commun.* **2017**, *221*, 383–418. [CrossRef]
15. Borschensky, C.; Gecse, Z.; Kraemer, M.; van der Leeuw, R.; Kulesza, A.; Mangano, M.; Padhi, S.; Plehn, T.; Portell, X.; Sekmen, S. LHC SUSY Cross Section Working Group. 2020. Available online: https://twiki.cern.ch/twiki/bin/view/LHCPhysics/SUSYCrossSections (accessed on 20 May 2022).
16. Sirunyan, A.M.; Tumasyan, A.; Adam, W.; Bergauer, T.; Dragicevic, M.; Escalante Del Valle, A.; Fruehwirth, R.; Jeitler, M.; Krammer, N.; Lechner, L.; et al. Search for supersymmetry in final states with two oppositely charged same-flavor leptons and missing transverse momentum in proton-proton collisions at $\sqrt{s} = 13$ TeV. *JHEP* **2021**, *4*, 123. [CrossRef]
17. Searches for new phenomena in events with two leptons, jets, and missing transverse momentum in 139 fb^{-1} of $\sqrt{s} = 13$ TeV pp collisions with the ATLAS detector. *arXiv* **2022**, arXiv:2204.13072.
18. Aaboud, M.; Aad, G.; Abbott, B.; Abdinov, O.; Abeloos, B.; Abidi, S.H.; AbouZeid, O.; Abraham, N.; Abramowicz, H.; Abreu, H.; et al. Search for electroweak production of supersymmetric states in scenarios with compressed mass spectra at $\sqrt{s} = 13$ TeV with the ATLAS detector. *Phys. Rev. D* **2018**, *97*, 052010. [CrossRef]
19. Search for direct top squark pair production and dark matter production in final states with two leptons in $\sqrt{s} = 13$ TeV pp collisions using 13.3 fb^{-1} of ATLAS data. *ATLAS-CONF-2016-076* **2016**. Available online: https://cds.cern.ch/record/2206249/files/ATLAS-CONF-2016-076.pdf (accessed on 12 May 2022).
20. Mangano, M. The So-Called MLM Prescription for ME/PS Matching. Fermilab ME/MC Tuning Workshop. 4 October 2002. Available online: http://www-cpd.fnal.gov/personal/mrenna/tuning/nov2002/mlm.pdf.gz (accessed on 1 June 2022).
21. Mangano, M.L.; Moretti, M.; Piccinini, F.; Treccani, M. Matching matrix elements and shower evolution for top-quark production in hadronic collisions. *JHEP* **2007**, *1*, 13. [CrossRef]
22. Cowan, G.; Cranmer, K.; Gross, E.; Vitells, O. Asymptotic formulae for likelihood-based tests of new physics. *Eur. Phys. J. C* **2011**, *71*, 1554. Erratum: *Eur. Phys. J. C* **2013**, *73*, 2501. [CrossRef]
23. Cowan, G. *Discovery Sensitivity for a Counting Experiment with Background Uncertainty*; tech. rep.; Royal Holloway: London, UK, 2012. Available online: http://www.pp.rhul.ac.uk/~cowan/stat/medsig/medsigNote.pdf (accessed on 27 May 2022).